Electronic structure of strained (La$_{0.85}$Ba$_{0.15}$)MnO$_3$ thin films with room-temperature ferromagnetism investigated by hard x-ray photoemission spectroscopy

Hidekazu Tanaka,[1,*] Yasutaka Takata,[2] Koji Horiba,[2] Munetaka Taguchi,[2] Ashish Chainani,[2] Shik Shin,[2] Daigo Miwa,[2]
Kenji Tamasaku,[2] Yoshinori Nishino,[2] Tetsuya Ishikawa,[2] Eiji Ikenaga,[3] Mitsuhiro Awaji,[3] Akihisa Takeuchi,[3] Tomoji Kawai,[1]
and Keisuke Kobayashi[3]

[1]*ISIR-Sanken, Osaka University, 8-1 Mihogaoka, Ibaraki, Osaka, 567-0047, Japan*
[2]*RIKEN/SPring-8, 1-1-1, Mikazuki-cho, Sayo-gun, Hyogo 679-5148, Japan*
[3]*JASRI/SPring-8, 1-1-1 Kouto, Mikazuki-cho, Sayo-gun, Hyogo 679-5198, Japan*
(Received 1 November 2005; published 6 March 2006)

We report the bulk sensitive hard x-ray ($h\nu$=5.95 keV) core level photoemission spectroscopy to investigate the intrinsic electronic structure of strained (La$_{0.85}$Ba$_{0.15}$)MnO$_3$ thin films. In a 20 nm thick well-strained film with strongly enhanced ferromagnetism, a new sharp satellite peak appeared at the low energy site of the Mn $2p_{3/2}$ main peak; whereas, a broader signal was observed for the unstrained film with 300 nm thickness. Cluster calculations revealed that the intensity corresponded to the density of the state at the Fermi level relating to the magnitude of the ferromagnetic order. The satellite intensity also agreed quantitatively with the square of the magnetization.

PACS number(s): 75.70.−i, 71.30.+h, 71.27.+a, 79.60.−i

I. INTRODUCTION

Perovskite manganite exhibits a rich variety of electric and magnetic properties including colossal magneto-resistance,[1] ferromagnetism with metallic conduction,[2] perfect spin polarization,[3] charge and/or orbital ordering[4] due to the strong coupling between spin, and charge and orbital (lattice) degrees of freedom.[5] Interestingly, we found that the tensile strain from the substrate stabilized the double exchange ferromagnetism on lightly doped (La$_{1-x}$Ba$_x$)MnO$_3$ thin films[6,7] and that ultrathin films, even those with a 5 nm thickness, displayed room-temperature ferromagnetism in comparison to a ferromagnetic Curie temperature (T_C) of 260 K in unstrained systems.[8] This feature could not be observed in other manganites and is also important in relation to applications pertaining to spintronic devices such as a ferromagnetic (La,Ba)MnO$_3$/Sr(Ti,Nb)O$_3$ p-n diode[9] and a ferromagnetic (La,Ba)MnO$_3$/Pb(Zr,Ti)O$_3$ field effect transistor[10] working at room temperature. In an effort to elucidate the origin of this enhanced ferromagnetism, information concerning the electronic structures of the films is essential, in addition to that of the lattice structure and electric and/or magnetic properties, and could lead to the development of strongly corrected electron and spin devices.[11]

Photoemission spectroscopy (PES) is a powerful and standard tool that has been utilized to investigate the electronic structure of materials such as manganites.[12–15] Nevertheless, the standard PES technique is very surface sensitive even if soft x-rays (SXs) with relatively high energy ($h\nu \sim 1$ keV) are used because of short mean free paths of the emitted low kinetic energy electrons. This technique sometimes yields contradictory results in relation to bulk physical properties. Recently, high-resolution PES studies using hard x-rays [(HX)$h\nu \sim 6$ keV] have been employed in the investigation of HfO$_2$ on Si,[16] GaN,[17] (Ga,Mn) N,[18] (V,Cr)$_2$O$_3$,[19] high T_C cuprate[19] and (La$_{1-x}$Sr$_x$)MnO$_3$,[20] and others,[21,22] making it possible to reveal the true bulk electronic structure up to depths of 5 nm to 10 nm.

We utilized bulk sensitive HX-PES in the investigation of (La,Ba)MnO$_3$ thin films with various film thicknesses that exhibited strain-enhanced ferromagnetism. We proposed a quantitative relationship between the Mn $2p$ core level HX-PES spectra and bulk nature (intrinsic) ferromagnetism in this system and revealed the origin of the enhanced ferromagnetism.

II. EXPERIMENTAL PROCEDURE

(La$_{0.85}$Ba$_{0.15}$)MnO$_3$ epitaxial thin films with thickness (t) corresponding to 300 nm, 20 nm, and 3 nm were deposited on etched 0.01 wt. % Nb-doped SrTiO$_3$ (001) single-crystal substrates using a pulsed laser deposition (PLD) technique. The detailed film formation conditions were mentioned in early reports.[6,7] Film structures were examined by x-ray diffraction and high-resolution transmission electron microscopy.[7] Examination by atomic force microscopy (AFM) confirmed its atomically flat surface.[8] The magnetic properties were measured using a superconducting quantum interference device (SQUID) magnetometer, and the electrical resistivity was measured using a four-probe method. From Fig. 1, which shows the dependence of magnetization on temperature, it was determined that the T_C of the films were 282 K for t=300 nm, 299 K for t=20 nm, and about 100 K for t=3 nm. This tendency depicting an enhancement in ferromagnetism was consistent with our previous reports.[6–8] Following *ex-situ* magnetization measurements, the films were transferred into a photoemission chamber with a base pressure of 10^{-8} Pa from air without any surface cleaning process. HX-PES measurements for the Mn $2p$ core level were performed at an undulator beam line[23–25] BL29XU of SPring-8. The experimental setup including beam line optics has been described elsewhere.[16,18] The excitation energy was set to 5.95 keV with a bandwidth of 70 meV. An electron energy analyzer (Gammadata Scienta Co., R4000-10KV) dedicated for HX-PES was used. The
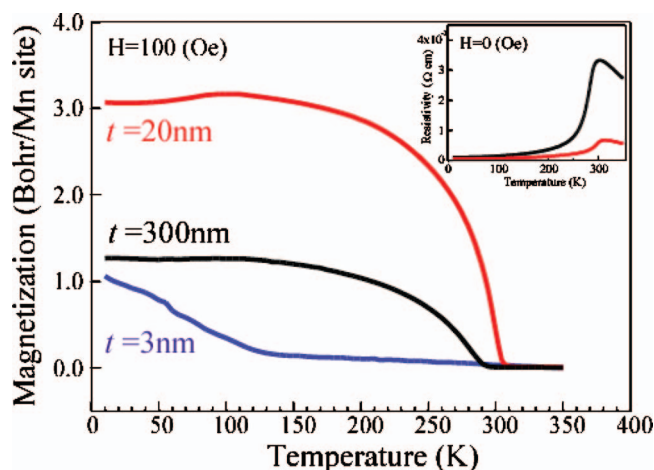
FIG. 1. (Color) Dependence of magnetization on temperature for $(La_{0.85}Ba_{0.15})MnO_3$ epitaxial thin films with thickness of 300 nm, 20 nm, and 3 nm on a Nb-doped $SrTiO_3$ (001) single-crystal substrate under a magnetic field of 100 Oe. T_C was defined as $dM(T)/dT=0$. The inset shows the dependence of resistivity on temperature for the 300 nm and 20 nm films.

total energy resolution was set to 160 meV and was confirmed by fitting the Fermi edge profile of an Au plate. The inelastic mean free path (IMFP) of the Mn 2p photoelectrons (kinetic energy: ~5.3 keV) in $(La,Ba)MnO_3$ was experimentally estimated as 6 nm. In an effort to verify the validity of the HX-PES, the core level SX-PES spectra were also measured at an undulator beam line BL17SU. The excitation energy was 1.44 keV and the IMFP was estimated as 1.5 nm.

III. RESULTS AND DISCUSSION

Figure 2 (a) shows the Mn 2p core level spectra of $(La,Ba)MnO_3$ thin films with $t=300$ nm by HX with an incident photon energy of 5.65 keV [spectrum (A)], $t=20$ nm films by HX with that of 5.65 keV [spectrum (B)], and $t=20$ nm films by SX with that of 1.44 keV [spectrum (C)]. In the core level spectra of (A) and (B) as measured by HX-PES, additional shoulder (satellite) structures appeared at the low binding energy side (about 639 eV) of the Mn 2$p_{3/2}$ main peak (about 641 eV), in comparison to the SX-PES spectrum (C) at low temperature. This dependence of satellite intensity on temperature was more clearly observed by HX-PES than by SX-PES for the $t=20$ nm film and indicated that HX-PES is superior to SX-PES in providing certain information relating to whole film (bulk) properties from an electronic structure standpoint.

Figure 2(b) shows the Mn 2$p_{3/2}$ HX-PES spectra at 28 K for $(La,Ba)MnO_3$ films with $t=300$ nm, 20 nm, and 3 nm. The satellite intensity of the $t=20$ nm film was much stronger than that of the $t=300$ nm film. This tendency corresponded to the observed enhancement in ferromagnetism of the 20 nm film with higher T_C and lower resistivity relative to the 300 nm film as shown in Fig. 1. For the $t=3$ nm film, where the ferromagnetism was strongly suppressed, no shoulder structure was observed. The observed variation in satellite intensity strongly corresponded to the magnitude of
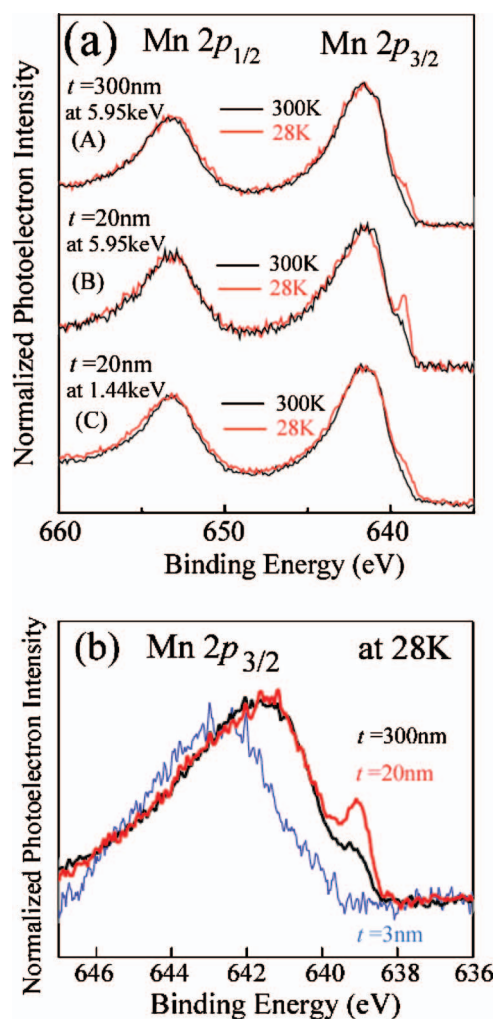

FIG. 2. (Color) (a) The Mn 2p core level spectra of $(La_{0.85}Ba_{0.15})MnO_3$ thin films with $t=300$ nm and $t=20$ nm by hard x-ray ($h\nu=5.95$ keV), and the spectrum measured by soft x-ray ($h\nu=1.44$ keV) for $t=20$ nm. (b) The Mn 2$p_{3/2}$ core level spectra of $(La_{0.85}Ba_{0.15})MnO_3$ thin films at 28 K with $t=300$ nm, 20 nm, and 3 nm.

the magnetization and metallicity of the $(La,Ba)MnO_3$ films with various thickness.

To make clear a quantitative relationship between ferromagnetism and satellite intensities, Fig. 3 shows the dependence of the Mn 2$p_{2/3}$ spectra on temperature for the $t=20$ nm film whose ferromagnetism was strongly enhanced. With increasing temperature from 28 K to 320 K, the satellite intensity systematically decreased and almost disappeared at 300 K, which corresponded to a T_C of 299 K. Above T_C of 300 K, quite weak and broad shoulder structure might be still considered, but its intensity is constant and independent from temperature change. This tendency was also confirmed during wide temperature change from 200 K−300 K for the different sample with T_C of 200 K as shown in Fig. 4. Therefore, rapid evolution of the satellite intensity seems to correspond to the evolution of ferromagnetism in the manganites. Taguchi *et al.*[19] and Horiba *et al.*[20] reported that satellite peaks were observed in the $(V,Cr)_2O_3$, high T_C cuprate, and $(La_{1-x}Sr_x)MnO_3$ thin film displaying
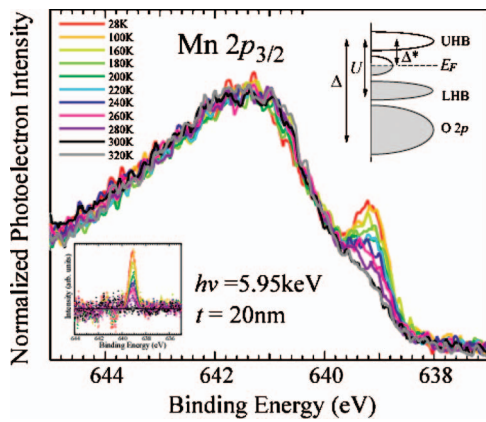
FIG. 3. (Color) Dependence of Mn $2p_{3/2}$ spectra on temperature for the $(La_{0.85}Ba_{0.15})MnO_3$ film with 20 nm thickness. The insets show the temperature variation part of the satellite peaks subtracted from the spectrum at 300 K and a schematic energy diagram of the valence band.

metallic state in the core level HX-PES spectra $(V:2p, Cu:2p, Mn:2p)$, and concluded that the satellite peak had originated from core-hole screening through evolution of density of the state at the Fermi level $[D(E_F)]$ using a cluster model calculation.[19] [In detail, in Fig. 2(a), the Mn $2p(3/2)$ main peak composed of a convolution of a many multiplet structures, leading to broader peak than satellite peak.[19] Although a satellite peak is also expected to appear near Mn $2p(1/2)$ peak, it should be broader than that near Mn $2p(3/2)$ peak on the basis of the calculation result.[19] Therefore, it might be difficult to discriminate.]

Now, we quantitatively propose the relationship between the HX-PES core level spectra and the ferromagnetism from its temperate dependence, and then compare the observed variation in satellite intensities to elucidate the enhanced ferromagnetism in $(La, Ba)MnO_3$ films. Figure 5 shows the dependence of the normalized satellite intensity $[I_S(T)]$ on temperature obtained by subtraction from the spectrum at 300 K. With developing ferromagnetic order and metallicity as the temperature decreased, $I_S(T)$ systematically increased. Cluster calculations which reproduced the observed spectra were
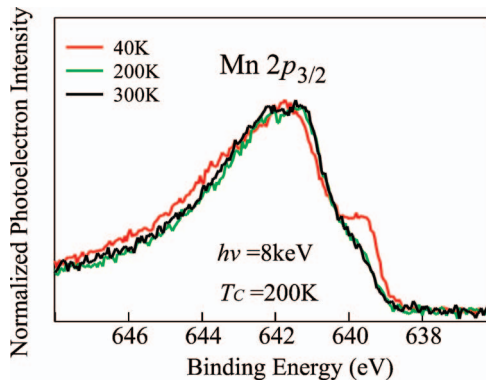

FIG. 4. (Color) Dependence of Mn $2p_{3/2}$ spectra on temperature for the $(La_{0.85}Ba_{0.15})MnO_3$ film with T_C of 200 K with 5 nm thickness on a 0.5 wt % Nb-doped $SrTiO_3$ (001) substrate by hard x-ray ($h\nu=8$ keV).
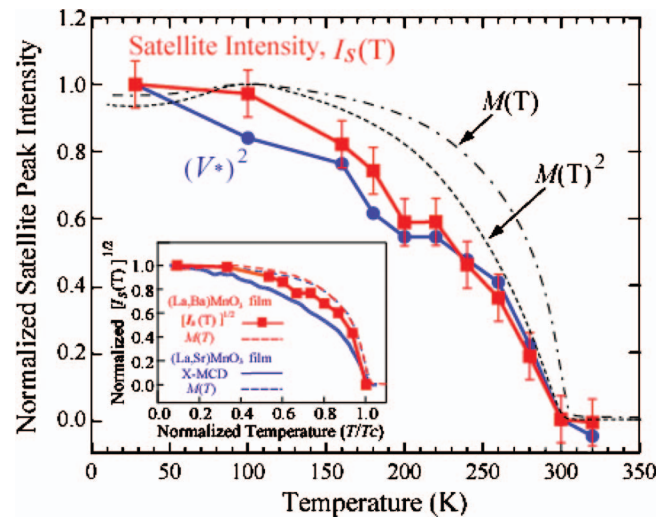

FIG. 5. (Color) Summarized dependence of normalized satellite intensities of the Mn $2p_{3/2}$ spectra $[I_S(T)]$, normalized hybridization parameter $(V^*)^2$, magnetization $[M(T)$ and $M(T)^2]$ on temperature. $I_S(T)$ and $(V^*)^2$ are normalized at 28 K (as 1.0) and 300 K (as 0). The inset shows the dependence of $\{I_S(T)\}^{1/2}$ and $M(T)$ on temperature for the $(La_{0.85}Ba_{0.15})MnO_3$ film ($t=20$ nm), and the dependence of the MCD signal and $M(T)$ on temperature for the $(La_{0.3}Sr_{0.3})MnO_3$ film. Data concerning the MCD signal and $M(T)$ for the $(La_{0.3}Sr_{0.3})MnO_3$ film were obtained from Ref. 27.

also employed to estimate the development of $D(E_F)$ (**C** state was introduced to represent a coherent metallic band at E_F, shown in inset of Fig. 3).[19,20] Three configurations were used for the initial states, namely $3d^4, 3d^5L$, where L is a hole in the ligand O $2p$ states, and $3d^5C$ which represents a charge transfer from the **C** state to the Mn $3d$ state. We fit the experimental spectra by changing only two parameters, the charge transfer energy between the Mn $3d$ and the **C** states (Δ^*) and the hybridization between the central Mn $3d$ orbitals and the **C** states (V^*). Except for these two parameters, all other parameter values were fixed (see Table I). The V^* and Δ^* parameters obtained are listed in Table I. These could reproduce the intensity and position of the satellite peaks of the experimental Mn $2p$ HX-PES spectra for the $t=20$ nm film at various temperatures. [Fitting curves are not shown. Effect of 20–30% $Mn^{4+}(d^3)$ was not included in calculation. It is noted that only the high binding energy side of Mn $2p3/2$ main peak does not match with the calculations. This difference is due to the Mn^{4+} derived state appearing at the high binding energy side of main peak with hole doping. See details in Ref. 20.]

It can be seen that V^* increased with developing ferromagnetic ordering as the temperature decreased. In detail, normalized $(V^*)^2$ plotted against temperature, as shown in Fig. 5, showed a consistency with the experimental behavior of $I_S(T)$. Mobile carriers existing at Fermi level $[D(E_F)]$ in the manganites causes ferromagnetism by the double exchange model,[26] so that we can imagine close relationship between the double exchange ferromagnetism and satellite intensity. Because V^* is strongly related to $D(E_F)$ and/or a transfer integral for conductive electrons, the following relationship of can be expected:

TABLE I. Fitting parameters (V^* and Δ^*) obtained by cluster calculations for the Mn $2p_{3/2}$ HX-PES spectra of the (La,Ba)MnO$_3$ thin film (20 nm) at various temperatures. Fixed parameters were the d-d Coulomb interaction of the Mn $3d$ states: $U=5.1$ eV, the charge transfer energy between the Mn $3d$ and ligand O $2p$ states: $\Delta=4.5$ eV, the hybridization between the Mn $3d$ and ligand O $2p$ states; $V=2.94$ eV, the crystal field splitting: $10Dq=1.5$ eV, the Coulomb interaction between the Mn $3d$ and Mn $2p$ core hole states: $U_{dc}=5.4$ eV, taken from Ref. 20.

Temperature (K)	V^* (eV)	Δ^* (eV)	Temperature (K)	V^* (eV)	Δ^* (eV)
28	0.4	0.8	240	0.33	0.8
100	0.38	0.8	260	0.32	0.8
160	0.37	0.8	280	0.29	1.0
180	0.35	0.8	300	0.25	1.1
200	0.34	0.8	320	0.24	1.2
220	0.34	0.8			

$$I_s(T) \approx \{M(T)\}^2. \tag{1}$$

The proposed equation (1) should be compared with experimental data to check its validity. As shown in Fig. 5, the experimental $I_S(T)$-T curve almost agrees well with the $\{M(T)\}^2$-T curve as measured by the SQUID magnetometer.

In an effort to check the matching to SQUID magnetization in more detail, we also employed a HX-PES experiment up to 10 keV photon energy, and obtained same $I_S(T)$-T curves. Therefore, using the proposed equation (1), we can discuss the electronic structure relating to double exchange ferromagnetism in the bulk part of the (La,Ba)MnO$_3$ film.

In another technique employed to evaluate the spin-related electronic structure for manganite, J. H. Park *et al.* reported on the in-site x-ray magnetic circular dichroism (X-MCD) in addition to surface sensitive spin-resolved PES analysis of a (La,Sr)MnO$_3$ film.[27] Compared with their X-MCD result concerning the temperature dependency as shown in the inset of Fig. 5, $\sqrt{I_S(T)}$ obtained from the HX-PES spectrum agrees well with $M(T)$. This is derived from the bulk sensitive nature of the HX-PES technique.

As discussed above, because the satellite intensity quantitatively corresponds to bulk magnetization, we go back to discussion on thickness dependence of electronic structure of (La,Ba)MnO$_3$ films. Although the origin of the enhancement of T_C in the (La,Ba)MnO$_3$ films with thickness from 5 nm to several hundred nanometers has been explained in terms of strain-induced changes in the lattice structure that lead to modification of the e_g band state,[6] some reports have argued that the enhancement of T_C originates from oxygen overdoping (namely cation deficiency) that causes additional hole doping.[28]

If the excess hole doping, namely the formation of Mn^{4+}, is introduced, the chemical shift of Mn $2p_{3/2}$ main peak toward higher energy should be detected as confirmed in the series of (La$_{1-x}$Sr$_x$)MnO$_3$ films with various Sr^{2+} doping ratio.[20] A comparison of the observed spectra for the 20 nm and 300 nm films shown in Fig. 2(b) revealed that the Mn $2p_{3/2}$ main peaks did not shift with decreasing film thickness, indicating that no additional hole doping was introduced.

Furthermore, the observed satellite peaks in Fig. 2(b) account for the development of V^* $[D(E_F)]$ with decreasing film thickness from 300 nm to 20 nm. Modification of e_g or-

bital state (decreasing the split between $d_{x^2-y^2}$ and $d_{z^2-r^2}$ orbitals and increasing bandwidth) by strain would enhance $D(E_F)$ and V^*, relating to double exchange ferromagnetism on the base of Eq. (1) without any additional Mn^{4+} formation.[6] As a result, the observed spectra of the 20 nm and 300 nm films deny an oxygen-overdoping scenario, but support a strain scenario. This also agrees with the result that the hole mobility estimated at 10 K increased from 5 cm^2/Vs to 50 cm^2/Vs with decreasing film thickness from 700 nm to 20 nm (T_C increased from 260 K up to 320 K) keeping almost constant carrier concentration[29] of 6×10^{20} cm^{-3}; whereas, it is expected that a cation deficiency causes a reduction of hole mobility and an enhanced hole concentration. As additional results, chemical composition analysis of (La,Ba)MnO$_3$ thin films with various film thickness elucidated that the Ba/La/Mn ratio is almost constant and independent from film thickness.[7] We also reported study on the structure and electrical transport properties of La$_{0.8}$Ba$_{0.2}$MnO$_{3+\delta}$ thin films prepared under various O$_2$ annealing conductions. This detailed investigation of the unit-cell volume strongly indicates the origin of the transition temperature enhancement of La$_{0.8}$Ba$_{0.2}$MnO$_{3+\delta}$ is essentially structural, and that the variation in carrier concentration induced by the variation in oxygen content generates only a minor effect.[30] These results also deny the oxygen-overdoping scenario.

Contrary to this, the Mn $2p_{3/2}$ main peak for the 3 nm film, which exhibited strongly suppressed ferromagnetism and insulating behavior, shifted to the higher binding energy side (about 643 eV), so that the origin of the suppressed ferromagnetism can be mainly accounted for by other additional factors such as a surface boundary layer,[3,27] and charge transfer between the film and substrate,[31,9] even though the film might be still strained. Namely, the enhancement of ferromagnetism in 300 nm and 20 nm thickness films originates from strain effect, but the suppression of ferromagnetism in 3 nm thickness film originates from mainly carrier modulation effect reflecting interfacial electronic structure.

IV. CONCLUSIONS

In conclusion, bulk sensitive core-level HX-PES was used to investigate (La$_{0.85}$Ba$_{0.15}$)MnO$_3$ strained thin films with

various thicknesses. The dependence of the satellite peak of the Mn $2p_{3/2}$ peak on film thickness systematically agreed with the ferromagnetic order in the bulk part of the films and revealed that V^* of the strained $(La, Ba)MnO_3$ films systematically evolved without additional Mn^{4+} formation in going from the 300 nm to 20 nm thick films, supporting a strain-induced ferromagnetism scenario from the viewpoint of electronic structure. The satellite intensity observed by HX-PES in the ferromagnetic $(La, Ba)MnO_3$ thin film corresponded to the bulk square of the magnetization on the basis of a model calculation that included charge transfer from the $D(E_F)$ to Mn $3d$ states.

Perovskite manganite film is considered to be one of the best candidates for use in the development of room temperature spintronics devices such as tunneling magnetoresistance devices[32] and ferromagnetic field effect transistors.[10] For these strongly corrected electron devices, it is essential that the electronic structure of the internal part of the film and interface part of the heterostructure far from the surface be elucidated. In particular, for ferromagnetic manganite, this technique makes it possible to estimate the electronic structure directly related to the magnetization at deep depths even without any surface treatment, and we believe that it can play an important role in the development of novel functional magnetic, electrical, and optical heterostructured devices constructed using transition metal oxides.

*Corresponding author. Email address: h-tanaka@sanken.osaka-u.ac.jp

[1] R. von Helmolt, J. Wecker, B. Holzapfel, L. Schultz, and K. Samwer, Phys. Rev. Lett. **71**, 2331 (1993).

[2] A. Urushibara, Y. Moritomo, T. Arima, A. Asamitsu, G. Kido, and Y. Tokura, Phys. Rev. B **51**, 14103 (1995).

[3] J. H. Park, E. Vescovo, H. J. Kim, C. Kwon, R. Ramesh, and T. Venkatesan, Nature (London) **392**, 794 (1998).

[4] H. Kuwahara, Y. Tomioka, A. Asamitsu, Y. Moritomo, and Y. Tokura, Science **270**, 961 (1995).

[5] M. Imada, A. Fujimori, and Y. Tokura, Rev. Mod. Phys. **70**, 1039 (1998).

[6] T. Kanki, H. Tanaka, and T. Kawai, Phys. Rev. B **64**, 224418 (2001).

[7] J. Zhang, H. Tanaka, T. Kanki, J. H. Choi, and T. Kawai, Phys. Rev. B **64**, 184404 (2001).

[8] T. Kanki, R. W. Li, Y. Naitoh, H. Tanaka, T. Matsumoto, and T. Kawai, Appl. Phys. Lett. **83**, 1184 (2003).

[9] H. Tanaka, J. Zhang, and T. Kawai, Phys. Rev. Lett. **88**, 027204 (2002).

[10] T. Kanki, Y. G. Park, H. Tanaka, and T. Kawai, Appl. Phys. Lett. **83**, 4860 (2003).

[11] C. H. Ahn, J. M. Triscone, and J. Mannhart, Nature (London) **242**, 1015 (2003).

[12] A. Chainani, M. Mathew, and D. D. Sarma, Phys. Rev. B **47**, 15397 (1993).

[13] T. Saitoh, A. E. Bocquet, T. Mizokawa, H. Namatame, A. Fujimori, M. Abbate, Y. Takeda, and M. Takano, Phys. Rev. B **51**, 13942 (1995).

[14] D. D. Sarma, N. Shanthi, S. R. Krishnakumar, T. Saitoh, T. Mizokawa, A. Sekiyama, K. Kobayashi, A. Fujimori, E. Weschke, R. Meier, G. Kaindl, Y. Takeda, and M. Takano, Phys. Rev. B **53**, 6873 (1996).

[15] K. Maiti, P. Mahadevan, and D. D. Sarma, Phys. Rev. Lett. **80**, 2885 (1998).

[16] K. Kobayashi, M. Yabashi, Y. Takata, T. Tokushima, S. Shin, K. Tamasaku, D. Miwa, T. Ishikawa, H. Nohira, T. Hattori, Y. Sugita, O. Nakatsuka, A. Sakai, and S. Zaima, Appl. Phys. Lett. **83**, 1005 (2003).

[17] K. Kobayashi, Y. Takata, T. Yamamoto, J. J. Kim, H. Makino, K. Tamasaku, M. Yabashi, D. Miwa, T. Ishikawa, S. Shin, and T. Yao, Jpn. J. Appl. Phys., Part 2 **43**, L1029 (2004).

[18] Y. Takata, K. Tamasaku, T. Tokushima, D. Miwa, S. Shin, T. Ishikawa, M. Yabashi, K. Kobayashi, J. J. Kim, T. Yao, T. Yamamoto, M. Arita, H. Namatame, and M. Taniguchi, Appl. Phys. Lett. **84**, 4310 (2004).

[19] M. Taguchi, A. Chainani, N. Kamakura, K. Horiba, Y. Takata, E. Ikenaga, T. Yokoya, S. Shin, K. Kobayashi, K. Tamasaku, Y. Nishino, D. Miwa, M. Yabashi, T. Ishikawa, T. Mochiku, K. Hirata, and K. Motoya, cond-mat/0404200 (unpublished).

[20] K. Horiba, M. Taguchi, A. Chainani, Y. Takata, E. Ikenaga, D. Miwa, Y. Nishino, K. Tamasaku, M. Awaji, A. Takeuchi, M. Yabashi, H. Namatame, M. Taniguchi, H. Kumigashira, M. Oshima, M. Lippmaa, M. Kawasaki, H. Koinuma, K. Kobayashi, T. Ishikawa, and S. Shin, Phys. Rev. Lett. **93**, 236401 (2004).

[21] J. J. Kim, H. Makino, K. Kobayashi, Y. Takata, T. Yamamoto, T. Hanada, M. W. Cho, E. Ikenaga, M. Yabashi, D. Miwa, Y. Nishino, K. Tamasaku, T. Ishikawa, S. Shin, and T. Yao, Phys. Rev. B **70**, 161315(R) (2004).

[22] H. Sato, K. Shimada, M. Arita, K. Hiraoka, K. Kojima, Y. Takeda, K. Yoshikawa, M. Sawada, M. Nakatake, H. Namatame, M. Taniguchi, Y. Takata, E. Ikenaga, S. Shin, K. Kobayashi, K. Tamasaku, Y. Nishino, D. Miwa, M. Yabashi, and T. Ishikawa, Phys. Rev. Lett. **93**, 246404 (2004).

[23] H. Kitamura, Rev. Sci. Instrum. **66**, 2007 (1995).

[24] H. Kitamura, J. Synchrotron Radiat. **7**, 121 (2000).

[25] K. Tamasaku, Y. Tanaka, M. Yabashi, H. Yamazaki, N. Kawamura, M. Suzuki, and T. Ishikawa, Nucl. Instrum. Methods Phys. Res. A **467/468**, 686 (2001).

[26] P. W. Anderson and H. Hasegawa, Phys. Rev. **100**, 675 (1955).

[27] J. H. Park, E. Vescovo, H. J. Kim, C. Kwon, R. Ramesh, and T. Venkatesan, Phys. Rev. Lett. **81**, 1953 (1998).

[28] P. Murugavel, J. H. Lee, J. G. Yoon, T. W. Noh, J. S. Chung, M. Heu, and S. Yoon, Appl. Phys. Lett. **82**, 1908 (2003).

[29] T. Kanki, T. Yanagida, B. Vilquin, H. Tanaka, and T. Kawai,

Phys. Rev. B **71**, 012403 (2005).

[30] M. Kanai, H. Tanaka, and T. Kawai, Phys. Rev. B **70**, 125109 (2004).

[31] M. Izumi, Y. Ogimoto, Y. Okimoto, T. Manako, P. Ahmet, K. Nakajima, T. Chikyow, M. Kawasaki, and Y. Tokura, Phys. Rev. B **64**, 064429 (2001).

[32] T. Obata, T. Manako, Y. Shimakawa, and Y. Kubo, Appl. Phys. Lett. **74**, 290 (1999).